Pilot plant reliability metrics for grinding and fast pyrolysis of woody residues

Jordan Klinger[a], Daniel L. Carpenter[b], Vicki S. Thompson[a], Neal Yancey[a], Rachel M. Emerson[a], Katherine R. Gaston[b], Kristin Smith[b], Michael Thorson[c], Huamin Wang[c], Daniel M. Santosa[c], Igor Kutnyakov[c]*

[a]Energy and Environment S&T, Idaho National Laboratory, 2525 Fremont Ave., Idaho Falls, ID 83415, USA

[b]National Bioenergy Center, National Renewable Energy Laboratory, 16253 Denver West Pkwy., Golden, CO 80401, USA

[c]Energy Processes & Materials Division, Pacific Northwest National Laboratory, 902 Battelle Blvd., Richland, WA 99352, USA

*daniel.carpenter@nrel.gov

ABSTRACT. Here we report on the effects of loblolly pine residue variability on material throughput, pilot plant uptime, operator intervention, product yield, and product quality for grinding, fast pyrolysis, and hydrotreating operations. Preprocessing throughput using a hammer mill varied between 31-48% of nameplate capacity (5 tons/hr). Grinder overloads in the size reduction step were more prevalent for lower ash and higher moisture materials. Fast pyrolysis throughput varied between 57-72% of nameplate capacity (20 kg/hr) and bio-oil yields varied

between 46-53% (feedstock carbon to oil, dry basis). During fast pyrolysis operations, downtime was caused by bridging in the feed and char removal systems and plugging in the condensation system. Cohesion of feedstock and char leading to system plugging was less frequent for higher ash feedstocks, and differences in condenser plugging behavior between high and low ash feedstocks were observed. The catalyst stability of the bio-oil stabilization step was strongly dependent on the sulfur content in the bio-oil, which was higher for the high-ash residue oils. Lower moisture content in the starting biomass was consistent with lower sulfur content in bio-oil. Yields and properties of hydrotreated fuel products showed minimal deference among the bio-oils.

KEYWORDS. Fast Pyrolysis, Biomass Preprocessing, Hydrotreatment Upgrading, Integrated Production, Pilot-Scale Operation, Process Reliability

SUPPORTING INFORMATION. Characterization methods and results for fast pyrolysis char and oil from the TCPDU.

INTRODUCTION. While biomass continues to show promise as a sustainable resource for generating renewable fuels and chemicals, consistent and reliable preprocessing, conveyance, and conversion operations, particularly for low-cost waste feedstocks, remains a critical technical problem for the emerging bioeconomy. Most first-generation biorefineries have been built around unique conversion technologies, with reactor systems constructed to enable chemistries that maximize the production of fuels and chemicals. Biomass feeding and handling systems have often been considered secondarily, resulting in significantly less effort expended on their up-front design and integration with downstream unit operations. Feeding and handling systems are often adapted or scaled down from other solids handling operations without a full

appreciation of the complexity of realistic biomass feedstocks, the potential variation in their chemical and physical attributes, or the impacts this variability has on the reliability of the overall process. Although generating knowledge vital to de-risking future industrial biofuels deployment, these pioneer systems have been unable to reliably feed material into conversion reactors, failing to achieve acceptable on-stream factors for economically viable operations. In 2016 the U.S. Department of Energy hosted a workshop to understand the underlying issues contributing to the relatively low operational reliability experienced by pioneer biorefineries and ways to overcome these barriers[1]. While the general lessons learned from these projects are available, detailed process performance data are not.

To illustrate the importance of process robustness, Figure 1 shows the estimated impact of on-stream factor on the minimum fuel selling price (MFSP) for a conceptual biomass thermal conversion process[2]. The increase in minimum selling price essentially reflects a cost penalty from unused installed capital, though it does *not* include any additional expense that would be needed to correct the underlying issues. The red line, taken from an often-referenced RAND Corporation study[3], indicates the average on-stream factor (49%) reported for pioneer process plants that handle solids.

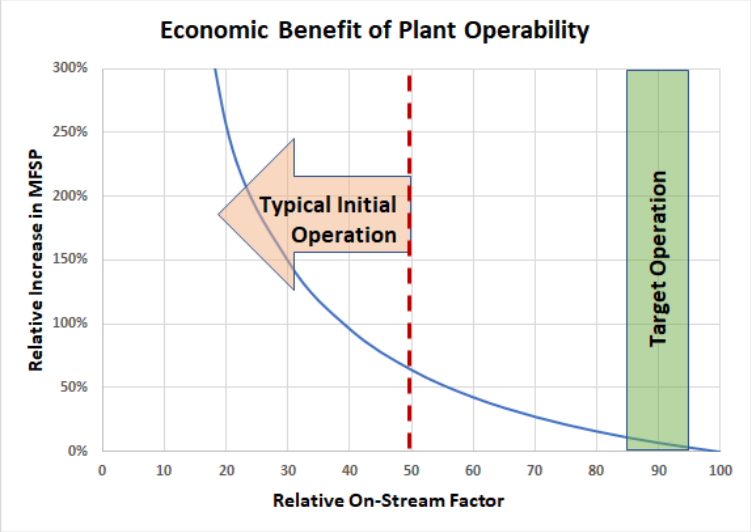

Figure 1. Estimated economic benefit (decrease in MFSP) due to increased biorefinery uptime. The blue curve is from a modeled biomass-to-fuels process via fast pyrolysis and hydrotreating; red line indicates the average performance of pioneer solids processing plants at one year as reported by Merrow et al.[2,3].

For an integrated process, there is a complex relationship between maximizing on-stream factor, controlling the quality of process intermediates, and maximizing the yield of final products, all of which are critical to the success of the overall process. For example, reducing biomass moisture increases drying costs, but increases grinding throughput and lowers grinding energy.[4,5] Previous studies have primarily focused on intermediate product yield and quality, with some consideration of process efficiency, economic, and sustainability as a function of feedstock type.[6-9] In particular, residues collected from responsibly and sustainably managed forests and plantations are of economic interest. The residues typically consist of branches, limbs, in addition to the top of trees where the stem width drop below six inches. Incorporation of residues, although highly variable, offer significant economic and sustainability advantages.[10,11] Understanding the impact of starting biomass variability on each of these factors, as well as the

interplay between individual unit operations, will be essential to successful process integration and large-scale deployment of biomass conversion systems.

The focus of this work was to understand the combined response of grinding, fast pyrolysis, and hydrotreating unit operations to commercially relevant variations in loblolly pine (clean pine and residues), specifically the ash and moisture contents. The objectives were to provide a quantitative measure of operational reliability, throughput, and conversion performance, and generate well-curated and publicly available experimental data. To maintain industrial relevance, commercial harvesting techniques were used, and grinding and pyrolysis experiments were performed at the pilot scale. The quality of the intermediate fast pyrolysis oil product was then assessed by measuring hydrotreating performance at the bench scale.

EXPERIMENTAL METHODS.

Experimental design. This study considered a 2x2 matrix of feedstock moisture and total ash, both of which have been demonstrated to have strong impacts on preprocessing and conversion, can be significantly variable in large scale biomass operations, and may be reasonably controlled in a commercial setting. Woody materials and residues are typically 50% moisture at harvest and must be dried to approximately 10% moisture for pyrolysis conversion. Drying is usually accomplished by *in situ* drying in the woods after harvest and a final drying step after size reduction. Drying is a costly step in terms of time (*in-situ* drying takes months), transportation (wet materials are heavier than dry), grinder energy (wet materials require more energy than dry), and energy required for convective drying. High moisture also results in inconsistent particle size distributions during grinding, an important factor for the pyrolysis step. Generally,

particle size increases with moisture, but decreases as screens become plugged, effectively reducing the screen opening[12].

Ash in biomass, or more accurately inorganic components (both physiological and extrinsic), has impacts on preprocessing operations such as accelerated equipment wear[13], and during thermal conversion operations by catalyzing decomposition reactions, such as cracking and dehydration to form light gases and water[14]. To examine the impacts of variable ash content, two types of woody biomass were sourced – clean debarked loblolly pine chips, and forest residues consisting of loblolly pine tree tops with branches. The four conditions were designated as low ash, low moisture (LALM); high ash, low moisture (HALM); low ash, high moisture (LAHM); and high ash, high moisture (HAHM). It should be noted that, while these designations are carried through the manuscript, the high and low moisture indicators have no practical meaning after the size reduction step since all samples were dried to <10% moisture content.

Three types of data were collected during these tests: (1) real-time process data for the various unit operations, such as motor current, temperature, and pressure; (2) observational data including process upsets, operator interventions, slowdowns, process downtime, and corrective actions taken; (3) detailed characterization of the feedstock and product streams. Throughputs were calculated for the main unit operations, using cumulative downtimes or slowdowns, for comparison to their nameplate capacity.

Forest residue sourcing. Clean, debarked, delimbed loblolly pine was harvested from Screven County, GA. Trees were 25 years old with a 9-inch diameter at breast height and an average height of 58 feet. Trees were harvested using a Tigercat 724G feller buncher and a Tigercat 630E grapple skidder. Whole trees were fed into a Peterson Pacific 5000H disc knife chipper using a

knuckle boom and flail chains to remove bark, limbs and needles. Chips were nominally 2 inches and average moisture at harvest was 51%. Loblolly pine whole trees and tree tops were obtained from Edgefield County, SC on March 26, 2018 from a 24-year-old planted stand. Trees were 11-inch diameter at breast height and 58 feet tall. Trees were harvested using a Cat 563D feller buncher, a CAT 535D grapple skidder and were fed by a CAT 559C knuckleboom loader into a Morbark 40/36 drum knife chipper. Nominal chip size was 2 inches and moisture at harvest was 49%. Both materials were shipped to INL and stored in uncovered bunkers until processing.

Feedstock preparation. Feedstocks were further processed at the Idaho National Laboratories (INL) Biomass Feedstock National User Facility (BFNUF, see Figure 2). Chips were fed by conveyor into a Vermeer HG-200 grinder (Pella, IA) fitted with a ¾ inch screen. After passing through the screen, the size-reduced woody feedstocks were fed via drag conveyor into a Baker Rullman (Watertown, WI) rotary drum dryer, model SD75-22 and dried to either 10% or 30% moisture. The dried materials were fed by drag conveyor into the 150 hp Eliminator hammermill second stage grinder (Bliss Industries, Ponca City, OK) and ground to pass a ¼ inch screen. The 30% moisture samples were dried a second time down to 10% moisture and loaded into supersacks for shipment to the National Renewable Energy Laboratory. Samples were collected prior to first stage grinding, after stage 1 grinding, after drying, after second stage grinding and prior to supersack loading. Supersack samples were analyzed for moisture content (drying for 24 hours at 105°C) and total ash content (750°C until constant weight was achieved).

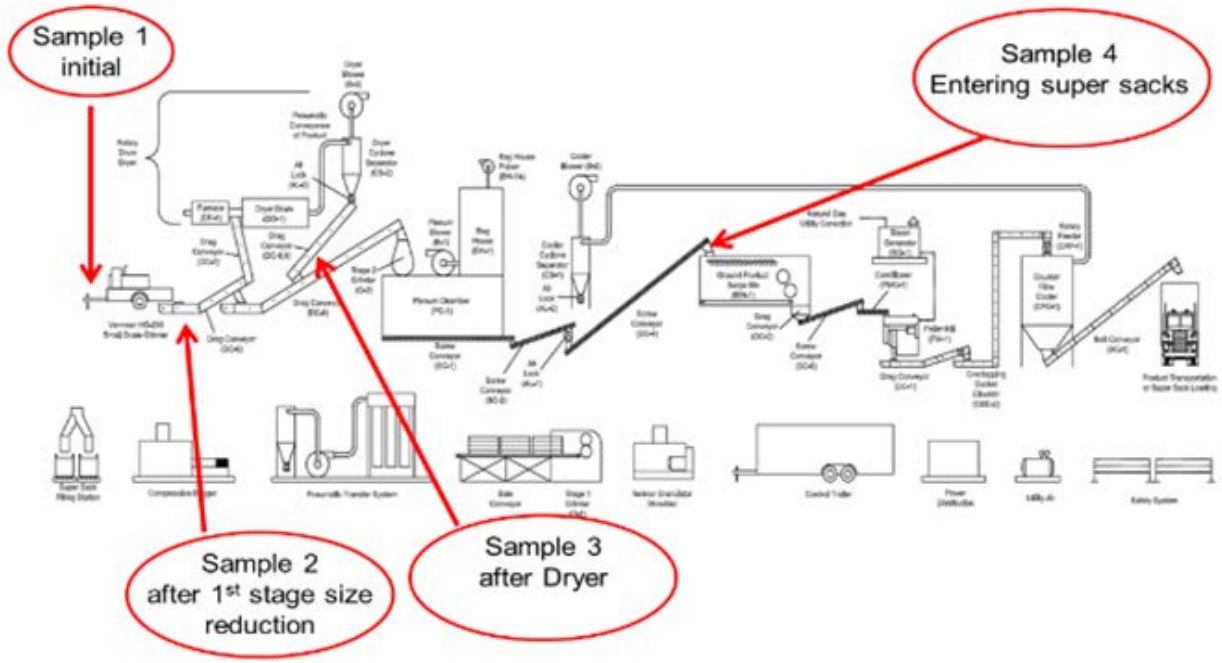

Figure 2. Schematic of INL's Biomass Feedstock National User Facility (BFNUF) used for biomass preprocessing (https://bfnuf.inl.gov/SitePages/Process%20Development%20Unit.aspx).

Feedstock characterization methods. Samples collected were analyzed for proximate and ultimate analysis using standard methods. Proximate analysis followed ASTM D3172-07, and ASTM D3176-09 was followed for ultimate analysis with a modification for biomass materials. Particle size distributions were measured and calculated using ASTM D4749-87 (2007). Samples were sent to Huffman Laboratories (Golden, CO) for elemental ash analysis using inductively coupled plasma – atomic emission spectroscopy for major and minor ash forming elements. In general, these procedures are done under the guidance of ASTM D3174, D3682, and D6349. Full compositional analysis was performed according to the Laboratory Analytical Procedures developed at NREL.[15] Loblolly pine characterization and preprocessing datasets are available in the Bioenergy Feedstock Library (bioenergylibrary.inl.gov).

Fast pyrolysis. Fast pyrolysis tests were carried out at the National Renewable Energy Laboratory's (NREL's) Thermal and Catalytic Process Development Unit (TCPDU). The TCPDU was configured for fast pyrolysis, which consisted of the following unit operations: feed transport system; entrained flow reactor; solids removal and collection; and liquid scrubbing, collection, and filtration (see Figure 3). The feeding system consists of a loss-in-weight feeder, three rotary valves, and a nitrogen eductor. Milled biomass was metered out of the hopper and into the eductor where pre-heated nitrogen transported the biomass to an entrained flow pyrolysis reactor. The reactor is a 30-meter (98 ft.) long by 3.81-cm (1.5 inch) diameter pipe with 12 independently controlled, electrically heated zones. For these experiments, the feed rate was 15 kg/h and the reactor temperature was 500°C. A back-pressure control valve maintained the pyrolyzer pressure at 60 kPa. The solids collection system consisted of two cyclonic separators in series, under which collection vessels accumulated the hot char. The char was then pneumatically conveyed to a nitrogen cooling vessel before being transferred to a collection drum. The drum was continuously weighed and, when full, removed and controllably passivated. The pyrolysis vapors exiting the cyclones were quenched by a liquid scrubber system, which consisted of a conical spray vessel for mixing hot vapors with dodecane scrubbing liquid to condense the vapors. This was followed by a gas-liquid separation vessel, 10-micron liquid filters, and a heat exchanger before entering a phase separator. This vessel allowed the bio-oil to settle for collection while recirculating the scrubbing liquid back to the scrubber vessels. Non-condensable gases from the separator (hydrogen, CH_4, CO, CO_2, and C_2+ hydrocarbons) were analyzed by NDIR and GC and sent to a thermal oxidizer.

The goal for these tests was to feed each biomass sample type long enough to observe multiple interventions of each type. The ultimate types and frequencies of potential interventions were not

known. However, based on previous experience, it was anticipated that the scrubber inlet would need to be cleared every 10-14 hours.

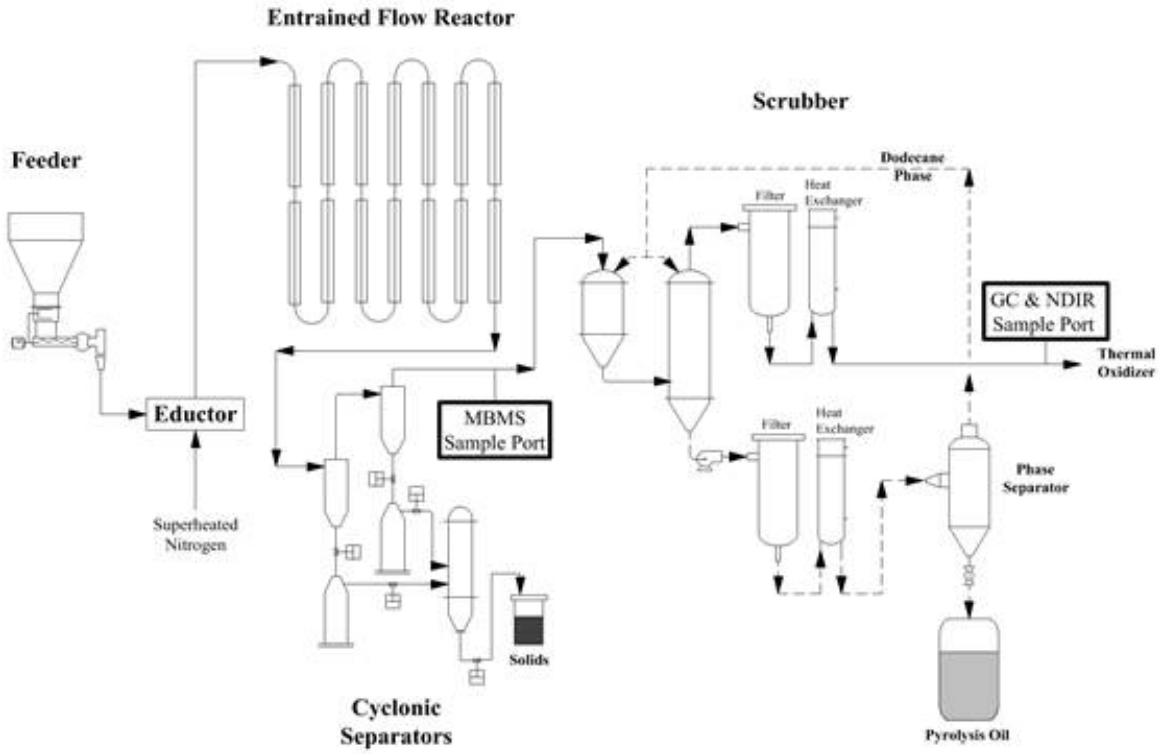

Figure 3. Process flow diagram of NREL's Thermal and Catalytic Process Development Unit (TCPDU) used for fast pyrolysis experiments (https://www.nrel.gov/bioenergy/tcpdu.html).

Pyrolysis product characterization. Liquid, gas, and solid pyrolysis product streams were analyzed by several techniques including proximate, ultimate, elemental ash, viscosity, density, titration, and GC-MS. These methods have been described in detail elsewhere[7] and are summarized in the Supporting Information (Tables SI-1 and SI-2).

Bio-oil upgrading. The bio-oils were upgraded to produce fuel range hydrocarbon using a two-step process as described by Elliot et al.[16] (see Figure 4). Bio-oil stabilization by hydrogenation

was carried out at ~140 ºC and 1800 psig with a reduced Ru/TiO_2 catalyst and LHSV of 0.20 h^{-1}. Details of the procedure can be found in Wang et al.[18] and major parameters are listed in Table 1. Stabilization tests were conducted between 80 and 160 hours on stream and the products at different times on stream for each bio-oil feed were combined into one sample. These samples formed two phases and were homogenized by adding 9.1 wt.% of methanol, which enabled steady feeding into the second hydrotreater system. Hydrotreating of the stabilized bio-oil was carried out at ~400 ºC and 1800 psig using a sulfided NiMo-based commercial hydrotreating catalyst. Detailed information about this process was reported previously[16,19] and major parameters are listed in Table 1. Each hydrotreating test was conducted between 80 and 120 hours on stream and steady-state products and outlet gas analysis data were collected in operating windows of 12 hours. Hydrogen consumption (g H_2 per g dry feed) was calculated based on the bio-oil flow rate and the difference of hydrogen inlet and outlet flowrates. The yield of oil and water products were determined by weight. The added methanol was assumed to have undergone hydrodeoxygenation to gases and water and, to ensure a methanol-free basis calculation, the associated hydrogen utilization was subtracted from the overall mass balance.

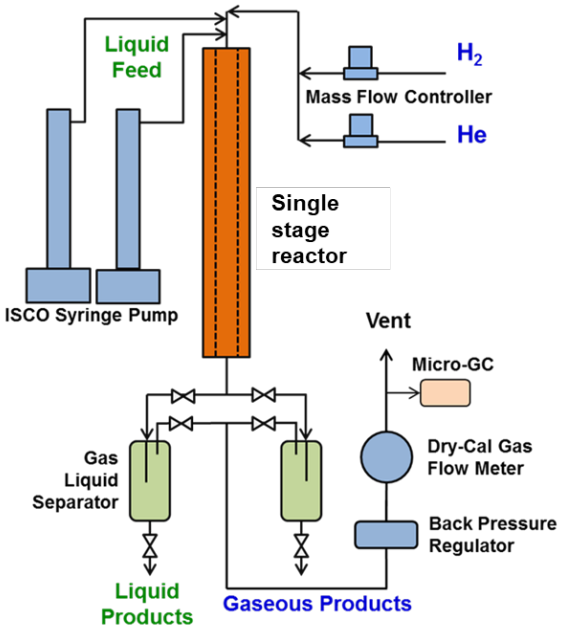

Figure 4. Schematic of PNNL's 40 ml two-stage hydrotreater system.

Table 1. Reaction parameters for upgrading of bio-oil via a two-step process.

	Stabilization Step	Hydrotreating Step
Catalyst	Ru/TiO_2	Supported NiMo based commercial catalyst
Catalyst pretreatment	300 °C in flowing H_2	400 °C in flowing H_2 and sulfiding agent (DTBDS in decane)
Temperature (°C)	140	400
Pressure (psig)	1800	1800
LHSV (h^{-1})	0.23	0.22 (excluding methanol)
H_2/bio-oil ratio (L/L)	2000	2100
Time on stream (hours)	80-160	80-120

Characterization of bio-oil, stabilized bio-oil, and hydrotreated products. The methods described for bio-oil analysis were also applied for the stabilized bio-oil and hydrotreated products for CHNOS content, moisture content, carbonyl content, CAN/TAN, and viscosity. Sulfur content in bio-oil was determined by inductively coupled plasma-optical emission

spectroscopy (ICP-OES). Density measurements were conducted on a Stabinger viscometer (Anton Paar SVM 3000) at 25 °C. Simulated distillation was conducted by using SimDis ASTM D2887 to estimate distribution of fuel fractions based on boiling point.

RESULTS AND DISCUSSION

Biomass preprocessing. Average values for moisture, ash, throughput, grinder energy and the geometric mean particle size for each feedstock are shown in Figure 5. Comparatively, the properties of residues (high ash) material that is comprised primarily of limbs, tops, etc. are significantly different to those of de-barked stem wood. Juvenile wood (tops, limbs, etc.) tend to have lower strength (thinner cell walls and greater fibril angle), lower cellulose content and more lignin.[20] The low moisture feedstocks averaged 11.5% and the high moisture 28.5% after grinding. The clean, debarked chips had an average ash content of 0.5% while the forest residues had a higher ash content of 1.7% due to the presence of needles, bark, smaller stems, and branches. As expected, the throughput was impacted by moisture content with the higher moisture materials having an average throughput of 34.5% of nameplate capacity (5 tons/hour) and the lower moisture materials with an average throughput of 47% of capacity. Figure 5 provides some insight into the reasons for the lower throughput as there were considerably more grinder overloads that occurred with the higher moisture materials. Grinder overloads required the operators to slow the system down to avoid overheating. Grinder energy had an inverse relationship with throughput where higher grinder energies were associated with lower throughput and lower energies with higher throughput, and represents a complex relationship between fundamental material deconstruction properties, the material attributes that impact deconstruction performance (such as moisture), as well as process efficiencies that manifest at higher throughputs. Moisture may have also had a slight impact on the mean particle size where

higher moisture materials were slighter larger than low moisture materials. Drier materials tend to shatter when hammermilled which can lead to smaller particle sizes.[21] Both at the particle scale and with bulk granular samples, the presence of moisture incorporated in the feedstock structure makes the sample more flexible, compressible, and overall more compliant.[21] Ash content did not appear to have any impact on throughput, grinder energy or particle size. Interestingly, Figure 5 does show that lower ash material resulted in more grinder overloads than higher ash material at given moisture content. This could be a result of the different plant tissues, and the relative abundance of plant tissues present in the various samples in addition to their comminution performance in the first stage of deconstruction.[20] An examination of particle size distributions (passing size distribution parameters for 10%, 50%, and 90% passing denoted as D10, D50 and D90 respectively) after the first grinder (sample point 3 in Figure 2) showed that while the D10 values were statistically the same for high ash versus low ash (0.875 ± 0.107 mm versus 0.944 ± 0.084 mm with 95% confidence intervals), the D90 values were significantly higher for the high ash materials (6.62 ± 0.080 mm 6.08 ± 0.186 versus mm with 95% confidence intervals). This suggests that a wider range of particle sizes results in fewer grinder overloads, although this needs to be verified with further testing.

It is important to note that the throughput of the system depends on its ‘nameplate capacity’, estimated to be nominally 5 tons/hour. In practice, conveyors, storage, and mill chamber capacity are limited by volume and not necessarily mass. Further, this capacity changes drastically with material type, moisture content, etc. and there are complications with defining a traditional design capacity that originated for a highly regulated processing feedstock (biomass is not). Rather than strict interpretation of this quantitative measure, the more impactful comparison is

between the qualitative differences illustrated by the varying values of this throughput factor, in addition to comparing the grinding energy and motor overloads with feedstock type as discussed.

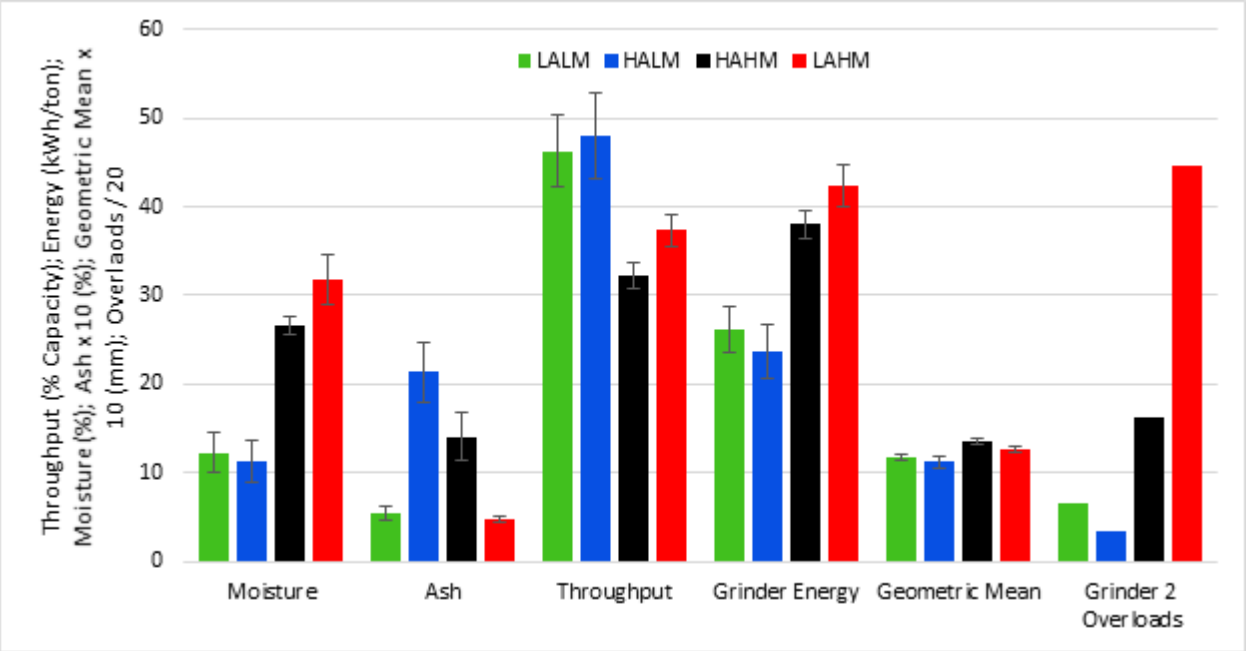

Figure 5. Average values for each condition tested of moisture, ash, throughput, grinder energy and geometric mean particle size. Error bars represent 95% confidence intervals calculated from a t-test.

Feedstock characterization results. Particle size distributions (D10, D50 and D90) for each feedstock after the second stage grinder (Sample point 4 in Figure 2) are shown in Figure 6.

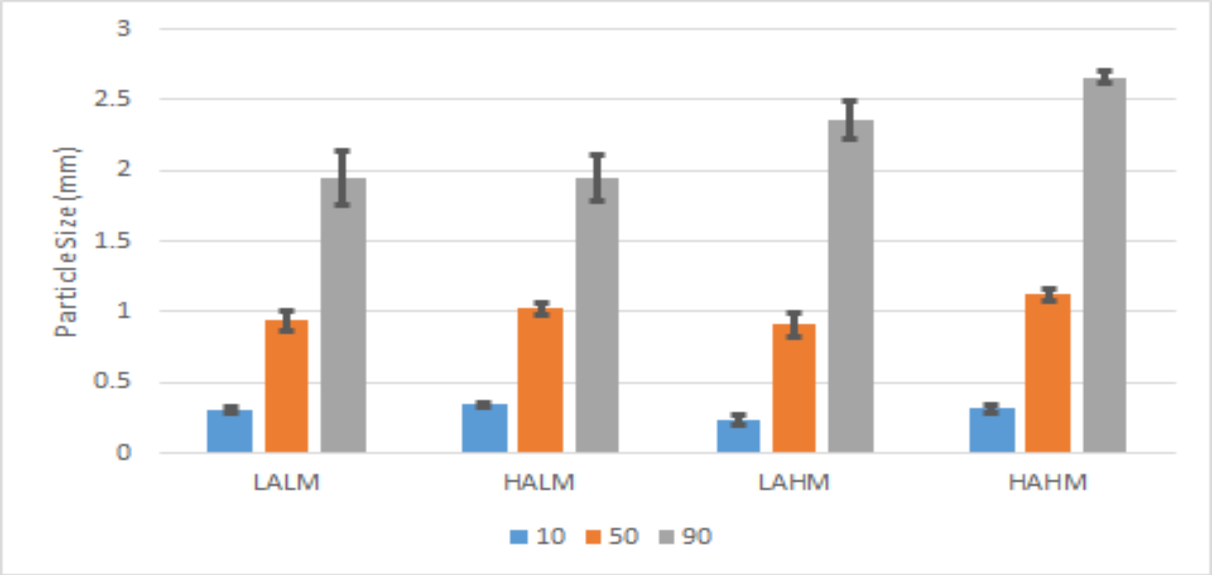

Figure 6. D10, D50, and D90 particle size data after the final grinding step. Error bars represent 95% confidence intervals as calculated by t-test.

Moisture content at the second grinder had a large impact on the D90 value with the higher moisture conditions having values of 2.36 ± 0.13 and 2.66 ± 0.04 mm compared to 1.95 ± 0.19 and 1.95 ± 0.16 mm for the low moisture conditions with the 95% confidence intervals shown. Moisture did not appear to have an impact on the D50 or D10 values. Unlike the material exiting the first stage grinder, ash did not appear to have an impact on the particle size distribution.

The proximate and ultimate analysis data for clean, debarked pine chips and forest residues after the final grinding step are shown in Figure 7. Forest residues have slightly lower levels of volatiles but slightly higher amounts of fixed carbon.

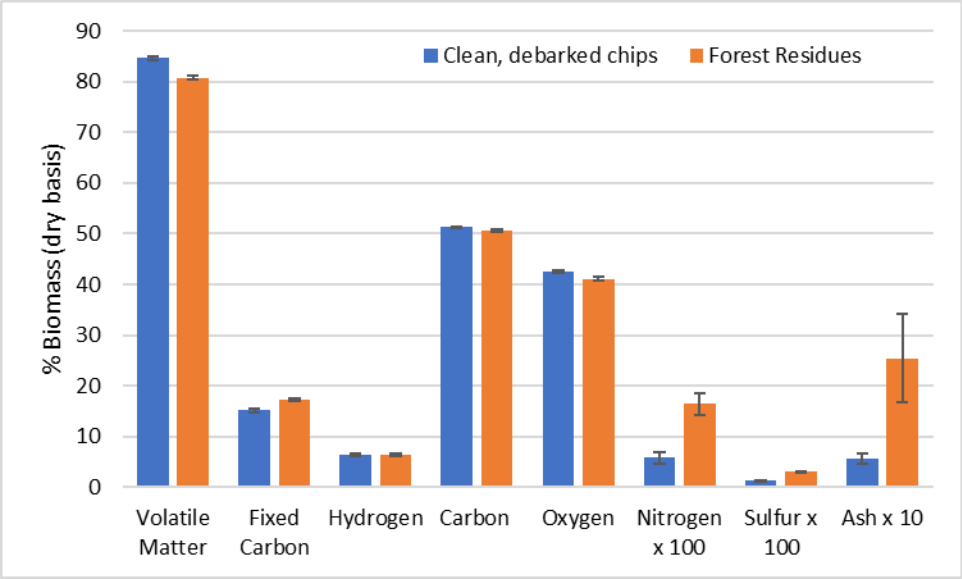

Figure 7. Comparison of proximate/ultimate data for low ash (clean, debarked pine) versus high ash (forest residues). Error bars represent 95% confidence intervals calculated by t-test.

There were no significant differences in hydrogen, total carbon or oxygen between residues and clean pine chips. Figure 7 shows values for nitrogen, sulfur and total ash. The total ash values are divided by 10 on the graph. Forest residues have significantly higher levels of nitrogen and sulfur compared to clean, debarked chips as well has having higher levels of total ash. Interestingly, the forest residues have been enriched in total ash compared to the forest residues at harvest which averaged 1.7% total ash. Elemental species for clean, debarked pine and forest residues are shown in Figure 8.

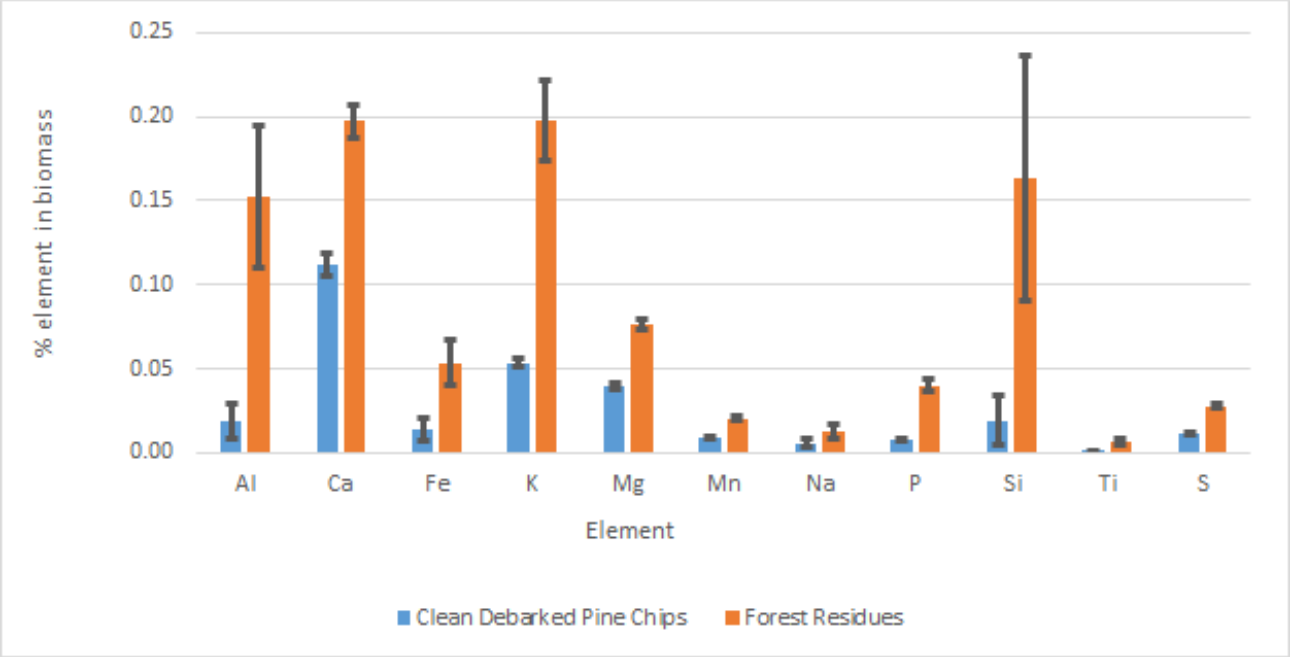

Figure 8. Elemental species comparison between clean, debarked pine and forest residues. Values presented are as a percentage of biomass. Error bars represent 95% confidence intervals as calculated by t-test.

Clean, debarked chips have much lower levels of all ash species compared to forest residues which is consistent with the overall lower levels of total ash present. Forest residues have 8-fold higher aluminum, 8.5-fold higher silica, 7.4-fold higher titanium and 3.9-fold higher iron. Since these are typical soil ash elements, this is indicative of higher amounts of soil contamination present in the forest residues as these materials are typically dragged on the ground and stored in piles during harvest and prior to chipping while the clean debarked pine is typically chipped directly into trucks for shipping. Forest residues also contain higher levels of the alkali and alkaline earth metals calcium, potassium, magnesium and sodium which are 1.75, 3.7, 1.9 and 2.1-fold higher than in the clean, debarked chips. These elements are primarily physiological and required by the trees during their growth process. These elements are particularly problematic for downstream pyrolysis and hydrotreating as they can catalyze decomposition reactions that effect

bio-oil quality[13]. Forest residues also have 2.3-fold higher sulfur than the clean pine chips and could cause problems during catalytic fast pyrolysis as sulfur is a known catalyst poison.

Fast pyrolysis results. Several operator interventions were required to maintain operations, resulting in operational downtime. Table 2 summarizes the interventions required for each process area and feedstock, as well as the average downtimes associated with each. Note that the high and low moisture designations (HM, LM) at this stage are considered proxy indicators of particle size distribution since all samples were dried to similar moisture levels prior to pyrolysis. The calculated on-stream factor, defined as the time-on-stream divided by the total experiment time, is shown in parenthesis. The interventions can be categorized into four process areas; biomass feed train, cyclone separators, char transfer system, condensation system (scrubber). Bridging and plugging in the feed train and char transfer system were frequent problems that required manual clearing of material. Occasional plugging at the cyclone inlet and scrubber inlet, caused by accumulation of condensed vapors and/or fine char, required stopping of feed and oxidation of the buildup. The two sections of the process were isolated from one another during respective oxidations so that the two shutdown events could be investigated independently.

There were significant variations in operator intervention type and frequency between feedstocks and, in some cases, between supersacks for a single feedstock type. All on-stream factors were similar except for the HALM material. This sample tended to flow better in the feed train and char collection system, which is reflected in the smaller number of interventions required. We hypothesize that the improved flow behavior of the HALM material is due to the more heterogeneous particle size and shape distributions observed for that material, which likely disrupts the cohesive tendencies that lead to bridging in more homogeneous materials. This is

consistent with previous anecdotal evidence observed at the labs, and consistent with the benefits seen with the use of flow aid additives in some bulk solids handling applications.

Table 2. Summary of process interventions required during fast pyrolysis tests.

System	Feed Train	Cyclones	Char	Scrubber
Description of intervention	Clear bridged biomass	Cyclone inlet oxidation	Clear bridged char	Scrubber inlet oxidation
Average downtime per intervention (h)	0.17	3.00	0.33	3.00
Feedstock (on-stream factor)	**Number of interventions required**			
LALM (0.57)	8	3	4	1
LAHM (0.59)	7	0	10	1
HALM (0.71)	4	0	2	2
HAHM (0.58)	9	2	4	2

A differential pressure (dP) measurement across the scrubber inlet was used as an indicator of material accumulation at this location. This is plotted as a function of time-on-stream for each of the four feedstocks in Figure 9, with steep rises in this measurement indicating plugging that required intervention. There were notable differences in the scrubber dP profiles between the high-ash and low-ash feedstocks. This suggests that differences in the nature of the deposited material resulted in distinct deposition behaviors. The vapor composition, molecular weight distribution, and entrained fine particles, all of which can vary with feedstock, will influence the apparent dew point. For instance, it is likely that reactive species in the vapor such as aldehydes, unsaturated ketones or esters, and phenols with reactive side groups (vinyl, aldehyde) initiate condensation reactions that lead to plugging.[22] Entrained fine particles can serve as nucleation sites for condensation. At this point, the physical and chemical mechanisms leading to these differences are unclear and warrant further investigation.

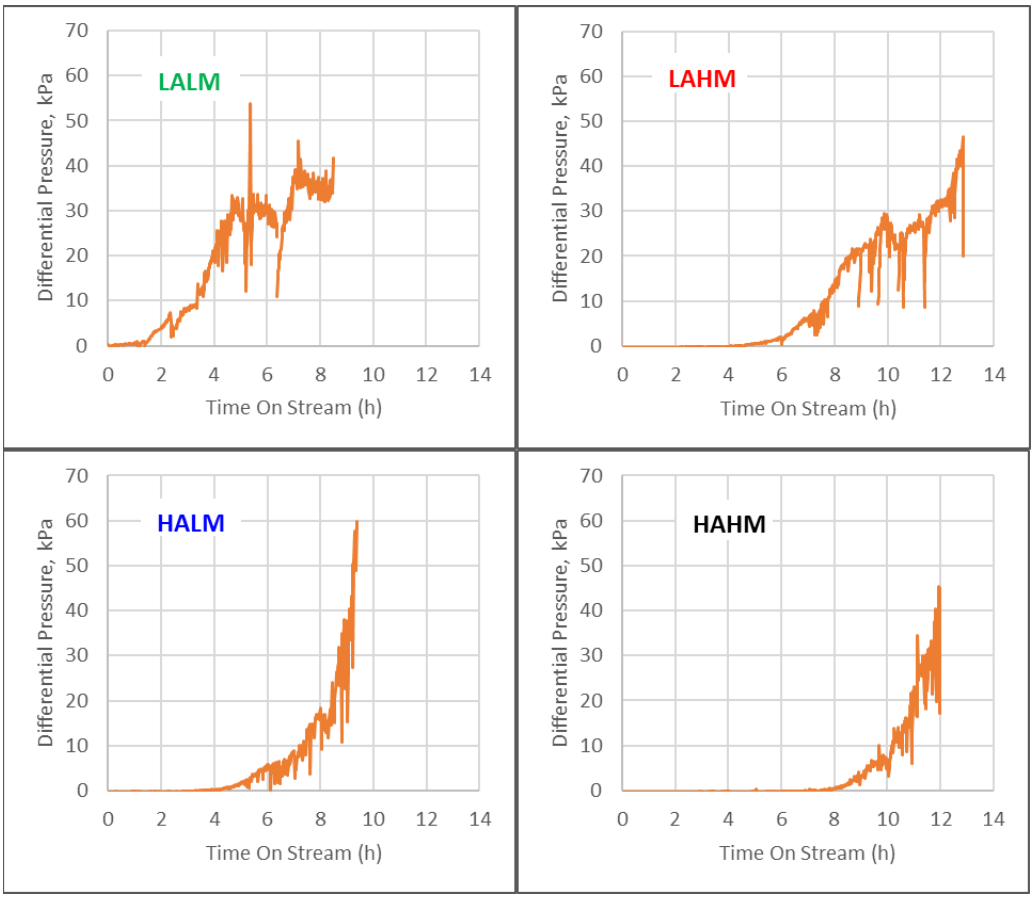

Figure 9. Differential pressure (dP) measurements across the TCPDU scrubber inlet as a function of time on stream for each feedstock.

The average bio-oil yields for the four feedstocks are shown in Figure 10 alongside the average measured throughputs (in T/d). Yields are reported on a dry, ash-free oil and biomass basis. As expected, the low-ash feedstocks produced more bio-oil than the high-ash materials, averaging 52.7% compared with 45.2%. The lower organic oil yield from the high-ash feedstocks was accompanied by higher water, char, and light gas production. Except for the LAHM material, at 84-88%, the mass balances were lower than typically measured in the TCPDU, which was likely due to the oil recovery being impacted by the large number of interventions.

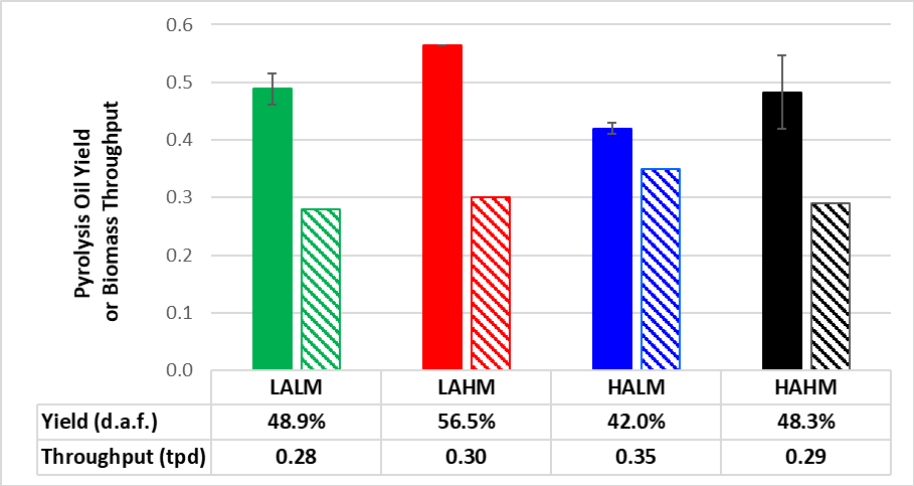

Figure 10. Pyrolysis oil yields (solid bars) and biomass throughputs (striped bars). Yields are $kg_{oil}/kg_{biomass}$ on a dry, ash-free oil basis. Throughputs are tons/day on an as-received basis and include downtime caused by interventions.

Table 3 shows pyrolysis product distributions and bio-oil analysis results from these experiments ("—" = below detection limits). The bio-oils were very similar in composition for all feedstocks except for the water content, which was higher for the high-ash feedstocks. The overall mass balances were 5-10% lower than is typically seen due to the required interventions, which can result in low recovered oil and reported yields. Characterization results for the fast pyrolysis char and gas from the TCPDU can be found in the Supplemental Information (Table SI-3). Char was collected and passivated using controlled air introduction prior to analysis. Gas analysis was by online gas chromatography and averaged for each feedstock. The high-ash feedstocks produced a higher ash char, as expected, and produced slightly less CO and more CO_2.

Table 3. Pyrolysis product distributions and bulk oil characterization results for the four feedstocks tested.

Feedstock	**LALM**	**LAHM**	**HALM**	**HAHM**
Product Yields (wt-% of biomass fed, wet basis)				

Total Liquid	62.3	69.6	54.1	60.2
Char	11.2	13.8	14.7	14.1
Gas	12.6	12.8	14.9	13.2
Mass balance	86.2	96.2	83.6	87.5
Oil Analysis (wt-% as received)				
Ash	<0.05	<0.05	<0.05	<0.05
C	43.1	44.0	41.1	42.2
H	7.4	7.5	7.5	7.5
N	0.1	0.1	0.2	0.2
O (by diff.)	49.5	48.5	51.3	50.1
Al	0.02	—	—	—
Ca	—	0.002	—	—
Fe	—	—	—	—
K	—	—	—	—
Mg	—	—	—	—
Na	0.022	0.003	0.004	0.007
P	—	—	—	—
Water	23.5	20.5	26.4	24.5
Carbonyl (mol/kg)	5.78	6.54	5.51	5.78
TAN (mg KOH/g)	68.3	67.9	66.1	67.3
Viscosity (cp, 40 °C)	31.8	41.7	21.4	30.1
Density (g/cm^3, 20 °C)	1.23	1.23	1.21	1.22

Units are wt-% as received except for TAN (mg KOH/g), Carbonyl (mol/kg), Viscosity (cp, 40 °C), Density (g/cm3, 20 °C).

GC-MS analysis of the bio-oil volatile fraction is shown in Figure 11. These results indicate a higher proportion of aldehydes produced from the high-moisture feedstocks (larger particle size after grinding) feedstocks. This could be indicative of less complete conversion of the larger particles under the same process conditions.[23] A lower concentration of sugar-derived species was produced from the high-ash feedstocks, which is likely due to their increased degradation from alkali metal-catalyzed depolymerization and dehydration reactions.

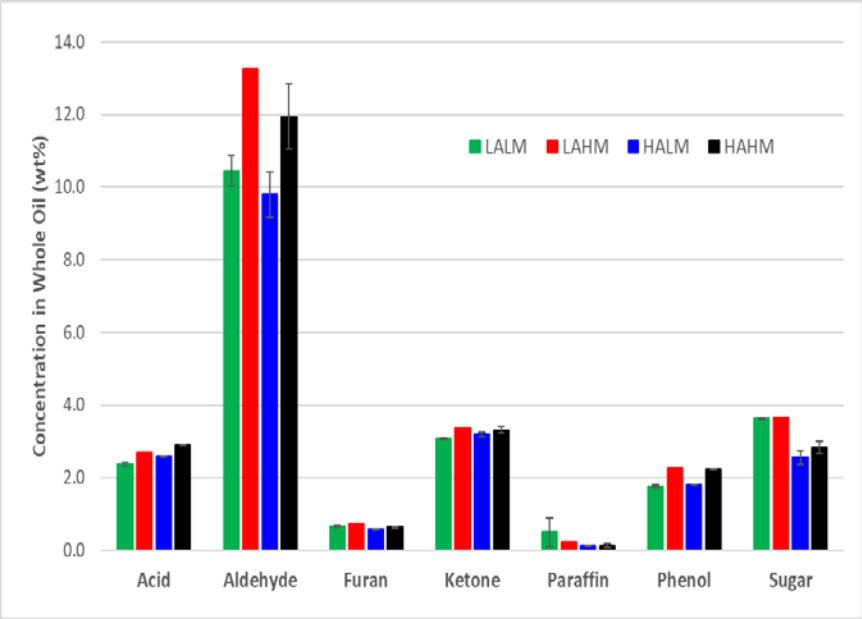

Figure 11. GC-MS analysis of major compound classes measured in bio-oils.

Hydrotreating results. Fast pyrolysis bio-oils are generally regarded as difficult to upgrade for production of hydrocarbon fuels because of their instability and chemical complexity. Several upgrading strategies have been developed with a focus on improving bio-oil stability through low temperature hydroprocessing, or catalytic fast pyrolysis, or separation approaches, prior to catalytic hydrotreating which removes oxygen from bio-oil, which substantially increases H/C ratio to product fuel range hydrocarbons.[24] Extensive progress has been made recent years in bio-oil hydrotreating and a significant development is a two-step process, including a low temperature stabilization step to hydrogenate reactive components in the bio-oil and a hydrotreating step to conduct more complete deoxygenation desired for hydrocarbon fuel production.[25] The development and performance of this two-step process was described in detail in a recent paper from PNNL.[25] Here, we use this two-step process to upgrade the bio-oils with a specific focus on product yield and quality and short-term catalyst stability with a timescale of 80-160 hours. The timescale is typical of most bio-oil upgrading regarding the stability of the

first step Ru/TiO_2 catalyst and reaching to steady-state for the second hydrotreating step and was used to get sufficient materials and data to generate rigorous information on product yield and quality and short-term catalyst stability. The long-term catalyst stability is not within the scope of this work; however, the previous work from PNNL demonstrated catalyst stability at longer time on stream for bio-oil stabilization and hydrotreating.[25,26] As described in detail in recent reports[16,18], the bio-oil stabilization step is intended to hydrogenate reactive species, such as carbonyl containing aldehydes, ketones, and sugar derived species, to alcohols and therefore stabilize the oil. This enables it to be hydrotreated without forming polymers that foul catalysts and plug reactors. Each bio-oil was hydrogenated over a Ru/TiO_2 catalyst at 140 ^oC in 1800 psi H_2 and the test was terminated if either sufficient products were produced or the carbonyl content in products was higher than 1.5 mmol/g. Figure 12 plots the change of H_2 consumption and carbonyl content of the stabilized bio-oil with time on stream. Clearly, a significant reduction of carbonyl content was achieved, from 5.0 - 5.5 mmol/g in bio-oil to 0.4 -1.8 mmol/g in product. However, the H_2 consumption decreased and carbonyl content increased with time on stream, indicating the deactivation of the catalyst. It was previously determined that sulfur poisoning of the Ru catalyst is the primary deactivation mechanism, followed by polymer formation fouling the catalyst, which could be significant when catalyst was losing hydrogenation activity because of sulfur poisoning[18]. Additionally, the deactivation trend of the four bio-oils showed a strong dependence on the sulfur content in bio-oils, which is shown in Table 4. The high sulfur bio-oil feeds (HAHM and HALM) deactivated the catalyst rapidly (75, and 82 ppm sulfur, respectively), whereas the lowest sulfur feed (LALM and LAHM) deactivated the slowest (19 ppm S), followed by the second lowest sulfur feed (HAHM, 29 ppm S). The secondary deactivation

mechanism, fouling by polymer formation, is much more complicated and is the topic of the current ongoing research.

These results clearly showed that both ash content and moisture content in biomass feedstock before grinding impacts the sulfur content in the produced bio-oil and consequently impacts lifetime of bio-oil stabilization catalysts in the upgrading process used here. Sulfur is known to be released from biomass at relatively low temperatures.[27] Biomass ash content, more specifically sulfur content (see Figure 8), showed a strong influence on sulfur content in bio-oil, consistent with the fact that bio-oil from high ash biomass (HALM and HAHM) contains ~50 ppm more than that from low ash biomass (LALM and LAHM). Moisture content of biomass feedstock before grinding appeared to slightly influence the sulfur content in the bio-oil, leading to a slightly (~10 ppm) higher sulfur content in the bio-oil. The causes of these differences are not clear.

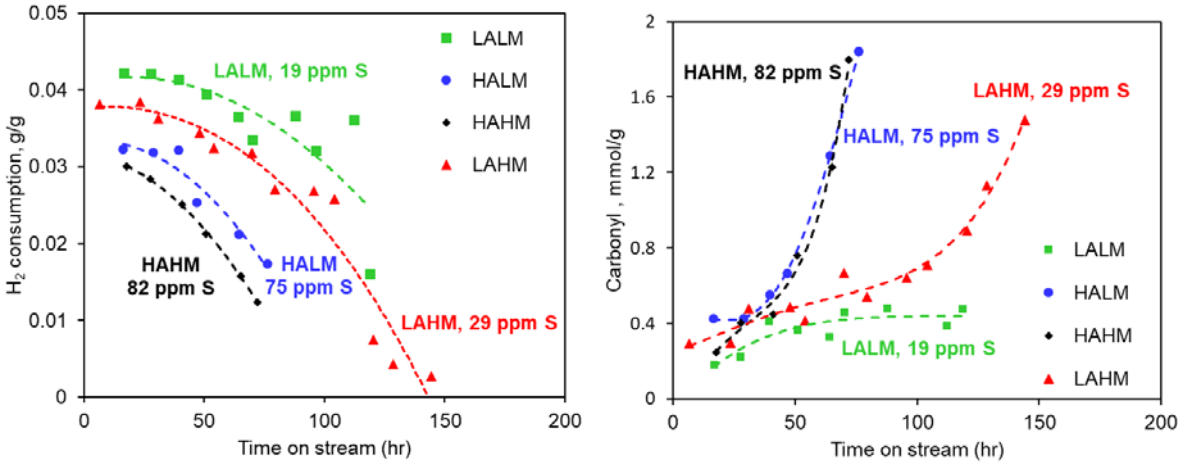

Figure 12. Hydrogen consumption (left) and carbonyl content in the product (right) as a function of time on stream during the stabilization of bio-oils over a Ru/TiO_2 catalyst.

No plugging issues were encountered while hydrotreating the stabilized oils over 80 to 120 hours on stream, which is expected as the carbonyl content in the stabilized bio-oil was low (0.4~0.5 mmol/g, Table 4). A steady state was achieved at time on stream over 60 hours and no catalyst deactivation was observed over the test period, consistent with a constant H_2 consumption, product yield, and hydrotreated oil density. Characterization of the steady state hydrotreated products is summarized in Table 4. In general, the four bio-oils showed minimal difference regarding hydrotreating performance and hydrotreated oil properties. The yield of hydrotreated oil ranged from 0.45-0.46 g/g bio-oil in dry basis. The hydrogen consumption only varied from 0.043 to 0.066 g H_2 per g of dry feed. The density, CHNOS analysis, and distillation fractions were very similar.

Table 4. Summary of hydrotreating results for the four bio-oil samples.

Bio-oil	**LALM**	**LAHM**	**HALM**	**HAHM**
Bio-oil				
Carbonyl content, mmol/g	5.5	5.4	5.1	5.2
S content, ppm	19	29	75	82
Density, g/ml	1.23	1.23	1.22	1.22
H_2O, wt/%	23.9	22.2	26.2	24.9
Stabilized bio-oil (combined, methanol excluded)				
Carbonyl content, mmol/g	0.37	0.41	0.51	0.53
H_2O, wt%	30.1	27.7	32.1	30.7
Hydrotreating performance (methanol excluded)				
Hydrotreated oil yield, g/g bio-oil, dry basis	0.447	0.445	0.453	0.464
Gas yield, g/g bio-oil, dry basis	0.234	0.241	0.194	0.210
Water yield, g/g bio-oil, dry basis	0.319	0.314	0.353	0.326
Carbon yield of hydrotreated oil, g/g	0.687	0.687	0.690	0.707
H_2 consumption, g/g bio-oil, dry basis	0.053	0.066	0.043	0.058
Hydrotreated oil				
Density, g/ml	0.800	0.813	0.816	0.815
C, wt.%, dry basis	86.9	86.4	87.0	86.9
H, wt.%, dry basis	13.1	13.1	13.1	13.1
N, wt.%, dry basis	<0.05	<0.05	<0.05	<0.05
O, wt.%, dry basis	<0.05	<0.05	<0.05	<0.05
S, wt.%, dry basis	<0.03	<0.03	<0.03	<0.03
H/C ratio, molar ratio	1.79	1.80	1.79	1.79

H_2O, wt%	0.04	0.02	0.04	0.04
Gasoline (IBP-150), wt.%, sim-dist	39.9	41.9	40.8	37.9
Diesel (150-350), wt.%, sim-dist	22.7	21.6	21.3	21.9
Jet (150-250), wt.%, sim-dist	23.2	23.1	22.4	23.0
Heavies (>350), wt.%, sim-dist	14.2	13.4	13.1	13.9

Overall process performance. For an integrated system it is important to understand the interactions and cost trade-offs between unit operations. Figure 13 (left) shows the average throughputs, in percent of nameplate capacity, for the grinding, pyrolysis, and combined operations (product of the two). Both unit operations had higher throughputs when processing the high ash, low moisture material. As described above, this is likely due to the physical heterogeneity of this material allowing it to flow better through these unit operations. It is important to note that the physical conveyance or flowability performance of the materials through unit operations is critical to operational reliability. Although flow through individual unit operation was not studied in this work, additional consortia efforts between the respective national laboratories is current investigating this issue heavily and is the topic of ongoing and forthcoming work. The combined performance further emphasizes this point. Figure 13 (right) shows the pyrolysis and hydrotreating yields for the four feedstocks, as well as the combined yield (product of the two). While the LAHM clearly shows a high yield in the pyrolysis step, the hydrotreating yield is relatively invariant to the bio-oils tested. Overall, the high moisture feedstocks show a slightly higher combined yield to hydrocarbon products. Feedstock variability clearly impacts each unit operation differently, even within a single species of biomass. This illustrates that overall system performance and cost implications are complex, and that integrated testing with realistic feedstocks is critical to developing robust processes.

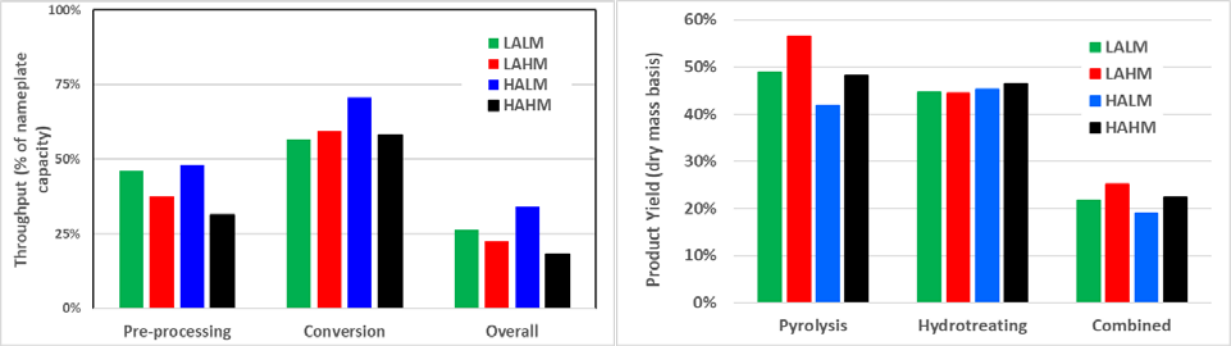

Figure 13. Left: summary of throughputs for grinding, pyrolysis, and overall system (product of the two). Right: Yields for fast pyrolysis, hydrotreating, and combined conversion to hydrocarbon blendstock ($kg_{product}/kg_{feed}$ at each step).

Statistical analysis. To provide greater understanding of the critical feedstock attributes impacting overall system performance and reliability, a subset of nine supersacks of loblolly pine chips and residues from the 2x2 experimental matrix discussed above that were processed in both pilot facilities were each labeled with four conversion processes efficiency metrics: 'On Stream', the ratio of the time on stream divided by the time on stream plus the downtime; 'Yield', the unoptimized liquid production efficiency produced at static operating conditions from the fast pyrolysis system; 'Char Removal', whether or not a run needed to be stopped to clean out either cyclones or char bridging; and 'Feed Train Bridging', whether or not there were bridging problems in the feed train during sample processing. For 'Yield' data was only available to label seven of the nine supersacks. As mentioned in the results for the pyrolysis conversion, there was significant variability between the individual supersacks within a single feedstock type, i.e., LALM, HAHM, etc. For the statistical analysis the supersacks were each considered unique samples representing the variability for the raw feedstock properties across the experimental matrix as biomass is very heterogeneous resource. The properties of the raw materials, including

proximate and ultimate composition factors, ash speciation, and particle size distribution factors, were assessed as potential explanatory variables for these four efficiency metrics. It should be noted that the chemical and physical variables of the raw materials used for this analysis are not all encompassing of possible property measurements for the raw material; however, these properties can give insight to the types of properties or act as proxies for other properties not currently or easily measured. A commercial statistics software package, JMP, was used to help identify statistical relationships between the raw feedstock properties and the conversion process efficiency metrics.

Because of the relatively small data set and the complexity of the performance metrics paired with complications in extracting material property and system operational performance relationships during large integrated operations, interpretation of trends is only appropriate; however, this analysis approach can provide trends that still be helpful in highlight avenues for process improvement. For the 'On Stream' metric, D50, geometric mean particle size, oxygen content, moisture, concentration of manganese, and D10 were all significantly ($p<0.1$) correlated to this performance metric when considered individually. As the 'On Stream' performance was primarily dominated by challenges with plugging in the feed train system and char transfer system, it is perhaps intuitive that descriptors of the particle size and moisture that largely govern the relative behavior of granular flow are correlated with performance. The oxygen and manganese contents relations are more abstract but could relate to the performance during thermal deconstruction or be proxy indicators of relative contents of fines or tissue fractions that are enriched with the respective constituents.

A multivariate least squares linear regression using a step-wise approach was used to quantify how much of the 'On Stream' variability could be explained and the relative explanatory strength

of each of the variables in relation to one another when added sequentially to the model (Fig. 14). The particle size parameter D50, negatively correlated, was identified as the strongest predictor variable with a single variable model root mean square error (RMSE) of 0.10 and R^2 of 0.55. The two samples with the largest D50 sizes (both from the debarked pine, one each high and low moisture) were among the three lowest 'On Stream' measures and exhibited issues for the char collection system and feed train system performance metrics. It is important to note that the D50 measures were strongly (R^2>0.8, positive) correlated to D10 (a representation of fines), but not that of the D90 or with distribution width (D90-D10) indicating that the heterogeneous nature of the debarked chips and residues is captured between D50 and D90 measures. Additionally, these regression results could be confounded by overall flow performance changes due to the magnitude of overall particle size, in addition to the size of the fine particles among other factors or interconnected factors not considered.

Moisture the second variable identified by the step-wise regression resulted in a cumulative RMSE of 0.092 and adjusted R^2 (to account for diminishing degrees of freedom and multicollinearity to D50) of 0.59; only a slight model improvement. Moisture was also negatively correlated to 'On Stream' performance. The moisture samples ranged from approximately 5.5-13%, with most samples clustered around 7.5-9.5%. The differences in moisture should only be considered impactful to the feed train system or as a proxy variable for relevant properties after the pyrolysis reaction. In this two-variable model, the analysis of variance yields an F-ratio of 6.83. While this is potentially significant, it does not improve upon the univariate model discussed above (F-ratio = 8.71). When the regression model was extended to include the next most impactful variable of ash content (cumulative RMSE 0.07, adjusted R^2=0.79) the ratio does improve upon the initial score (to 10.8). The next four variables

suggested in the step-wise approach, Fe_2O_3, hydrogen content, geometric mean particle size, and MgO, resulted in further decreases of the F-ratio (not included in Figure 14).

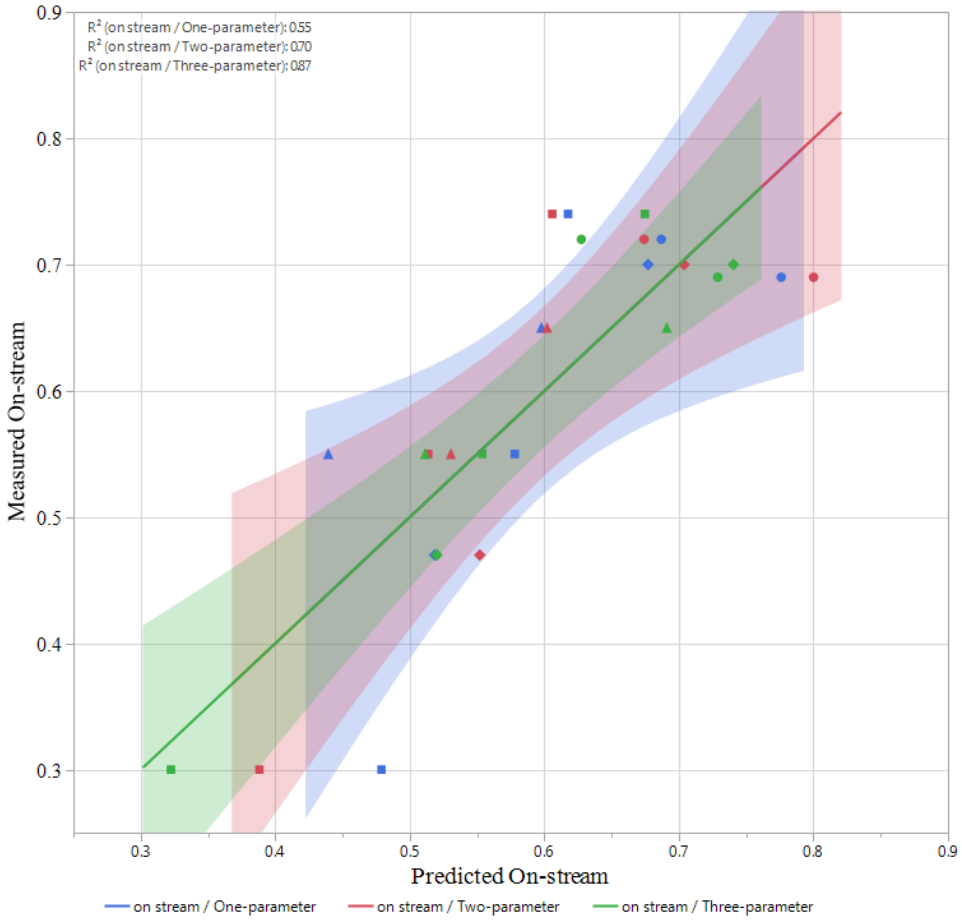

Figure 14. Measured and predicted 'On-stream' based on one-, two-, and three-parameter models. Square symbols are from LALM runs, circles represent HALM, diamonds represent HAHM, and triangles represent LAHM. The colors correspond to the respective regression model.

As with the 'On Stream' performance, a similar regression was performed on the measured, unoptimized yield from the pyrolysis of feedstock. The parameters identified in order of model

contribution strength were MgO (RMSE 0.053, R^2=0.53), D90 (cumulative RMSE 0.024, adjusted R^2=0.88), SiO_2 content (cumulative RMSE 0.006, adjusted R^2=0.99), Fe_2O_3, and TiO_2. The first parameter, MgO, appeared to differentiate the tests based on gross yield or material quality where the high ash runs tended toward lower yield compared to the debarked pine. Whereas many of the material attributes between the pine samples were similar, it is perhaps expected that a feedstock 'quality' parameter (discussed more fully below) is critical to differentiate yield performance. Figure 15 shows a similar prediction plot with results of several stepwise regression models with varying numbers of model parameters.

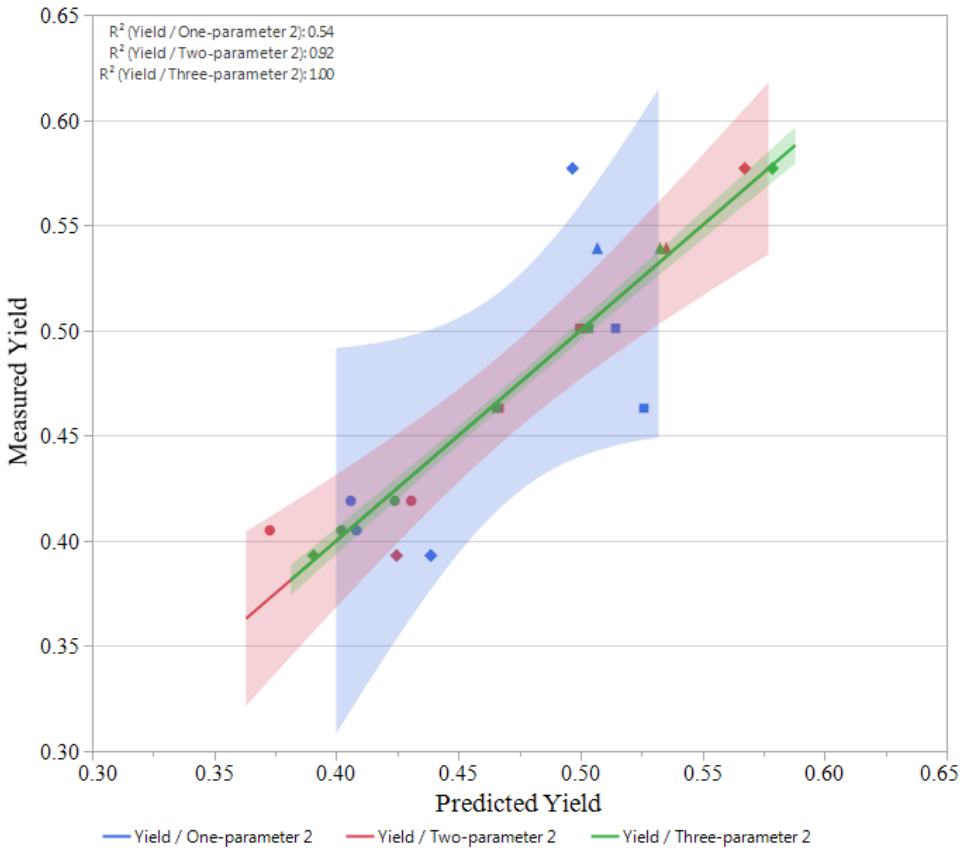

Figure 15. Measured and predicted 'Yield' based on one-, two-, and three-parameter models. Square symbols are from LALM runs, circles represent HALM, diamonds represent HAHM, and triangles represent LAHM. The colors correspond to the respective regression model.

In a separate principle component analysis of the pine samples, it was found that the difference in the MgO content was most drastic for the portion of whitewood in the sample compared to the other ideally orthogonal, and comparatively more similar contents in the components of bark, twigs, needles, etc. that are more abundant in the high-ash residue samples. The other identified significant inorganic constituents could be due to similar functions. In fact, when a two-parameter nominal logistics model was constructed based on MgO and SiO there was a 100% accuracy and ideal confusion matrix in prediction of the 2x2 matrix case in assignment of the 'LALM', 'LAHM', 'HAHM', and 'HALM' classifications. The SiO_2 content was higher in the high-ash samples, while MgO tended to higher contents in the low-ash materials. This nominal logistics approach was applied in a more general sense to a larger set of 55 unique samples and resulted in a 95% prediction accuracy among the 'high' (forest residues) and 'low' (debarked stem wood) ash classifications. For reference, this was as accurate as if the total ash was used in a logistic model for the same prediction. If the MgO is used alone, the only false assignment of a classification was allotting one low-ash, high-moisture sample as a low-ash, low-moisture preparation. This is an interesting result and indicated that various gross material fractions or material quality levels might be separable based on measurements of specific components.

During operation binary responses were recorded for the initial feed train system referred to as 'Feed Train Bridging' (Yes, bridging occurred during a run causing shutdown or No: bridging did not occur to an extent requiring shutdown) and the char collection system referred to as 'Char Removal' (Yes: char formation resulted in shutdown or No: char formation did not result in shutdown) to further describe unit operation upsets. For these binary conversion process efficiency metrics, a response screening methodology was used to identify the most impactful material attributes; however, as the data was limited, a good fit was not obtained for either

metric. The characteristics with the best description of these binary variables were titanium content (p-value 0.002) and D90 (p-value 0.03) for 'Char Removal' and nitrogen content (p-value 0.004), sodium (p-value 0.02), and total halogens (p-value 0.03) for the 'Feed Train Bridging'. For the char case, titanium is indicative of the presence of soil ash and the presence of fines, while D90 represents oversize particles. If fines and soil ash partition to char, this may explain these results. Having large amounts of oversized particles could be indicative that these particles are not completely reacting and ending up in the char phase (mentioned above). For the 'Feed Train Bridging' response screening, both sodium and halogens are linked to soil ash, although sodium is also a physiological element in plants. Further, the halogens are typically present in living plant tissues for nutrient membrane transport and retention and could be indicative of different types or qualities of plant tissues present in the samples that lead to process issues. Soil ash is typically present in the fines fraction and could contribute to bridging and plugging in flow systems. Nitrogen is typically indicative of proteins being present in biomass. These proteins are present in varying levels among the different plant tissues, and could indicate confounding impact of plant tissue origin, performance in size reduction and overall thermomechanical properties, and thus impact the overall system as a result of being sub-optimal for the design specification. As stated above, these factors and those described in the 'On Stream' and 'Yield' performance would require more validation to determine causal relationships.

Concluding Remarks. Operational reliability issues were highlighted for a representative biomass-to-fuel process and showed that grinding, pyrolysis, and hydrotreating steps were impacted differently by the feedstock variability. Preprocessing throughput (using multistage size reduction with hammer mills in series) varied between 31-48% of nameplate capacity (5

tons/hr). Grinder overloads in the size reduction step were more prevalent for lower ash and higher moisture materials. Fast pyrolysis throughput varied between 57-72% of nameplate capacity (20 kg/hr) and bio-oil yields varied between 46-53% (feedstock carbon to oil, dry basis). During fast pyrolysis operations, downtime was caused by bridging in the feed and char removal systems and plugging in the condensation system. Cohesion of feedstock and char leading to system plugging was less frequent for higher ash feedstocks, and differences in condenser plugging behavior between high and low ash feedstocks were observed. The catalyst stability of the bio-oil stabilization step was strongly dependent on the sulfur content in the bio-oil, which was higher for the high-ash residue oils. Lower moisture content in the starting biomass was consistent with lower sulfur content in bio-oil. The yields and properties of hydrotreated fuel products were similar among the four bio-oils. A detailed multivariate regression analysis and nominal logistics modeling approach showed that bio-oil yield is well predicted by MgO, D90, and SiO_2 content and that feedstock gross material fractions or quality levels might be separable based on measurements of specific components. These results highlight that understanding the impact of starting biomass variability on each unit operation and the interplay between them will be essential to economic and sustainable large-scale deployment of biomass conversion systems.

Author Contributions

The manuscript was written through contributions of all authors. All authors have given approval to the final version of the manuscript.

ACKNOWLEDGMENT

This work was authored in part by the National Renewable Energy Laboratory, operated by Alliance for Sustainable Energy, LLC, for the U.S. Department of Energy (DOE) under Contract No. DE-AC36-08GO28308; DOE Idaho Operations Office Contract DE-AC07- 05ID14517; and

DE-AC05-76RL01830 with Pacific Northwest National Laboratory. Funding provided by U.S. Department of Energy Office of Energy Efficiency and Renewable Energy, Bioenergy Technologies Office. The views expressed in the article do not necessarily represent the views of the DOE or the U.S. Government. The U.S. Government retains and the publisher, by accepting the article for publication, acknowledges that the U.S. Government retains a nonexclusive, paid-up, irrevocable, worldwide license to publish or reproduce the published form of this work, or allow others to do so, for U.S. Government purposes. The authors thank NREL pilot plant operators Tim Dunning, Katie Gaston, Chris Golubieski, Ray Hansen, Rebecca Jackson, Matt Oliver, Marc Pomeroy, and Kristin Smith; Steve Phillips for MFSP vs. on-stream time analysis; Ed Wolfrum for technical advice.

REFERENCES

(1) U.S. Dept. of Energy, Biorefinery Optimization Workshop Summary Report, **2016**, DOE/EE-1514, https://www.energy.gov/sites/prod/files/2017/02/f34/biorefinery_optimization_workshop_summary_report.pdf.

(2) Jones, S.; Meyer, P.; Snowden-Swan, L.; Padmaperuma, A.; Tan, E.; Dutta, A.; Jacobson, J.; Cafferty, K. Process design and economics for the conversion of lignocellulosic biomass to hydrocarbon fuels: Fast pyrolysis and hydrotreating bio-oil pathway, **2013**, Technical Report PNNL-23053, DOI:10.2172/1126275.

(3) Merrow, E.; Phillips, K.; Myers, C. Understanding Cost Growth and Performance Shortfalls in Pioneer Process Plants, **1981,** RAND Corporation, R-2569-DOE, https://www.rand.org/pubs/reports/R2569.html.

(4) Yancey, N.; Tumuluru, J.; Wright, C. Drying, grinding and pelletization studies on raw and formulated biomass feedstocks for bioenergy applications. *J. Biobased Mater. Bio.* **2013**, *7*, 549-558, DOI:10.1166/jbmb.2013.1390.

(5) Pace, D.; Yancey, N. Biomass Feedstock PDU Project: Biomass Comminution Study. **2014**, Technical Report INL/EXT-14-31058.

(6) Howe, D.; Westover, T.; Carpenter, D.; Santosa, D.; Emerson, R.; Deutch, S. Field-to-fuel performance testing of lignocellulosic feedstocks: an integrated study of the fast pyrolysis-hydrotreating pathway, *Energy Fuels* **2015**, *29,* 3188-3197, DOI:10.1021/acs.energyfuels.5b00304.

(7) Carpenter, D.; Westover, T.; Howe, D.; Deutch, S.; Starace, A.; Emerson, R.; Hernandez, S.; Santosa, D.; Kutnyakov, I.; Lukins, C. Catalytic Hydroprocessing of Fast Pyrolysis Oils: Impact of Biomass Feedstock on Process Efficiency, *Biomass & Bioenergy*, **2017**, *96*, 142-151, DOI:10.1016/j.biombioe.2016.09.012.

(8) Meyer, P.; Snowden-Swan, L.; Rappé, K.; Jones, S.; Westover, T.; Cafferty, K. Field-to-Fuel Performance Testing of Lignocellulosic Feedstocks for Fast Pyrolysis and Upgrading: Techno-economic Analysis and Greenhouse Gas Life Cycle Analysis, *Energy Fuels,* **2016**, *30,* 9427-9439, DOI:10.1021/acs.energyfuels.6b01643.

(9) Dupuis, D; Grim, G.; Nelson, E.; Tan, E.; Ruddy, D.; Hernandez, S.; Westover, T.; Hensley, J.; Carpenter, D. High-Octane Gasoline from Biomass: Experimental, Economic, and Environmental Assessment, *Applied Energy,* **2019**, *241*, 25-33, DOI:10.1016/j.apenergy.2019.02.064.

(10) Adom, F.; et al. Supply chain sustainability analysis of fast pyrolysis and hydrotreating bio-oil to produce hydrocarbon fuels. **2016**, No. ANL/ESD-15/2 Revision 1. Argonne National Lab. (ANL), Argonne, IL (United States), DOI:10.2172/1249552.

(11) Cai, Hao, et al. Supply Chain Sustainability Analysis of Renewable Hydrocarbon Fuels via Indirect Liquefaction, Fast Pyrolysis, and Hydrothermal Liquefaction: Update of the 2016 State-of-Technology Cases and Design Cases. **2017**, No. ANL-17/04. Argonne National Lab. (ANL), Argonne, IL (United States), DOI:10.2172/1346567.

(12) Tumuluru, J.; Yancey, N.; McCulloch, R.; Fox, C.; Conner, C.; Hartley, D.; Dee, M.; Plummer, M. Biomass Engineering: Size reduction, drying and densification of high moisture biomass. Feedstock supply and logistics platform, *DOE, Project Peer Review, US. Department of energy, Bioenergy Technologies Office*, **2017**, DOE/EE-1014, https://www.energy.gov/sites/prod/files/2017/05/f34/fsl_tumuluru_1222.pdf.

(13) Lacey, J.; Aston, J.; Thompson, V. Wear properties of ash minerals in biomass. *Front. Energy Res.* **2018**, *6*, 1-6, DOI:10.3389/fenrg.2018.00119.

(14) Wang, K.; Zhang, J.; Shanks, B.; Brown, R. The deleterious effect of inorganic salts on hydrocarbon yields from catalytic pyrolysis of lignocellulosic biomass and its mitigation. *Applied Energy*, **2015**, *148*, 115-120, DOI:10.1016/j.apenergy.2015.03.034.

(15) Sluiter, J and Sluiter, A. Summative mass closure: Laboratory analytical procedure (LAP) review and integration, **2011**, National Renewable Energy Laboratory: Golden, CO. NREL/TP-510-48087, https://www.nrel.gov/docs/gen/fy11/48087.pdf.

(16) Elliot, D.; Hart, T.; Nuenschwander, G.; Rotness, L.; Olarte, M.; Zacher, A.; Solantausta, Y. Catalytic hydroprocessing of fast pyrolysis bio-oil from pine sawdust. *Energy Fuels,* **2012**, *26,* 3891-3896, DOI:10.1021/ef3004587.

(17) Elliot, D.; Wang, H.; French, R.; Deutch, S.; Iisa, K. Hydrocarbon liquid production from biomass via hot-vapor-filtered fast pyrolysis and catalytic hydroprocessing of the bio-oil. *Energy Fuels,* **2014**, *28,* 5909-5917, DOI:10.1021/ef501536j.

(18) Wang, H.; Lee, S.; Olarte, M.; Zacher, A. Bio-oil stabilization by hydrogenation over reduced metal catalysts at low temperatures. *ACS Sustainable Chem. Eng.,* **2016**, *4,* 5533-5545, DOI:10.1021/acssuschemeng.6b01270.

(19) Griffin, M.; Iisa, K.; Wang, H.; Dutta, A.; Orton, K.; French, R.; Santosa, D.; Wilson, N.; Christensen, E.; Nash, C.; Van Allsburg, K.; Baddour, F.; Ruddy, D.; Tan, E.; Cai, H.; Mukarakate, C.; Schaidle, J. Driving towards cost-competitive biofuels through catalytic fast pyrolysis by rethinking catalyst selection and reactor configuration. *Energy Environ. Sci.,* **2018**, *11,* 2904-2918, DOI:10.1039/C8EE01872C.

(20) Kretschmann, D., Bendtsen, A. Ultimate tensile stress and modulus of elasticity of fast-grown plantation loblolly pine lumber. *Wood Fiber Sci.*, **1992**, *24*, 189–203, https://wfs.swst.org/index.php/wfs/article/download/810/810.

(21) U.S. Dept. of Energy, Feedstock supply system design and analysis. **2014** Idaho National Laboratory. INL-EXT-33227, https://bioenergy.inl.gov/Reports/Feedstock%20Supply%20System%20Design%20and%20Analysis.pdf.

(22) Diebold, J. A Review of the Chemical and Physical Mechanisms of the Storage Stability of Fast Pyrolysis Bio-Oils. **2000**, National Renewable Energy Laboratory, NREL/SR-570-27613, DOI:10.2172/753818.

(23) Ansari, K., Arora, J., Chew, J., Dauenhauer, P., Mushrif, S. Fast Pyrolysis of Cellulose, Hemicellulose, and Lignin: Effect of Operating Temperature on Bio-oil Yield and Composition and Insights into the Intrinsic Pyrolysis Chemistry. *Ind. Eng. Chem. Res.*, **2019**, *58*, 15838-15852, DOI:10.1021/acs.iecr.9b00920.

(24) Albrecht, K., Olarte, M., Wang, H. Upgrading Fast Pyrolysis Liquids. In *Thermochemical Processing of Biomass: Conversion into Fuels, Chemicals, and Power;* Brown, R. Ed.; Wiley Online Library, **2019**: 2nd Edition, pp 207-255, DOI:10.1002/9781119417637.ch7.

(25) Zacher, A., Elliot, D., Olarte, M., Wang, H., Jones, S., Meyer, P. Technology advancements in hydroprocessing of bio-oils. *Biomass and Bioenergy*, **2019**, *125,*151-168, DOI:10.1016/j.biombioe.2019.04.015.

(26) Olarte, M., Zacher, A., Padmaperuma, A., Burton, S., Job, H., Lemmon, T., Swita, M., Rotness, L., Neuenschwander, G., Frye, J., Elliot, D. Stabilization of Softwood-Derived Pyrolysis Oils for Continuous Bio-oil Hydroprocessing, *Topics in Catalysis,* **2016**, *59,* 55-64, DOI:10.1007/s.11244-015-0505-7.

(27) Saleh, S., et al. Release of chlorine and sulfur during biomass torrefaction and pyrolysis. *Energy Fuels,* **2014**, *28,* 3738-3746, DOI:10.1021/ef4021262.

For Table of Contents Use Only

TOC/ABSTRACT GRAPHIC.

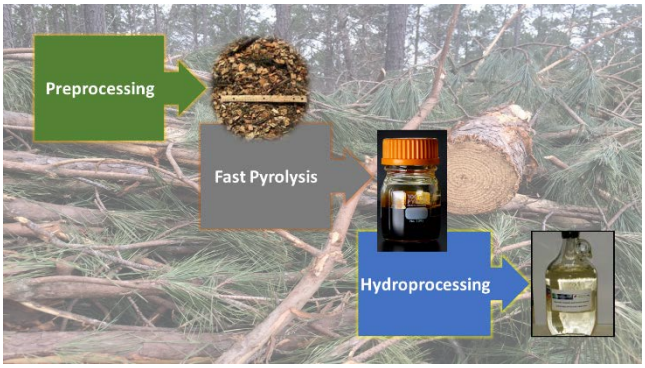

SYNOPSIS. This work explores reliability issues surrounding conversion of loblolly pine resources to renewable fuels with respect to feedstock quality.